Original paper

Gladkovskyite, $MnTlAs_3S_6$, a new thallium sulfosalt from the Vorontsovskoe gold deposit, Northern Urals, Russia

Anatoly V. KASATKIN[1]*, Emil MAKOVICKY[2], Jakub PLÁŠIL[3], Radek ŠKODA[4], Nikita V. CHUKANOV[5], Sergey Y. STEPANOV[6], Atali A. AGAKHANOV[1], Fabrizio NESTOLA[7]

[1] *Fersman Mineralogical Museum of Russian Academy of Sciences, Leninsky Prospekt 18-2, 119071 Moscow, Russia; anatoly.kasatkin@gmail.com*
[2] *Department of Geoscience and Resource Management, University of Copenhagen, Østervoldgade 10, DK-1350, Copenhagen K, Denmark*
[3] *Institute of Physics, Academy of Sciences of the Czech Republic v.v.i, Na Slovance 1999/2, Prague 8, 182 21, Czech Republic*
[4] *Department of Geological Sciences, Faculty of Science, Masaryk University, Kotlářská 2, 611 37, Brno, Czech Republic*
[5] *Institute of Problems of Chemical Physics, Russian Academy of Sciences, Chernogolovka, Moscow region, 142432 Russia*
[6] *Zavaritsky Institute of Geology and Geochemistry, UB RAS, Akademika Vonsovskogo str. 15, 620016 Yekaterinburg, Russia*
[7] *Dipartimento di Geoscienze, Università di Padova, Via Gradenigo 6, I-35131, Padova, Italy*
* *Corresponding author*

Gladkovskyite (IMA2018-098), $MnTlAs_3S_6$, is a new sulfosalt from the Vorontsovskoe gold deposit, Sverdlovsk Oblast', Northern Urals, Russia. The new mineral occurs in limestone breccias cemented by abundant realgar, orpiment, baryte and pyrite, as well as minor clinochlore, fluorapatite, quartz and talc. Gladkovskyite forms long-prismatic crystals and grains up to 0.2 mm; it has dark cherry-red color and red streak. It is transparent with adamantine luster. The Vickers microhardness is 94 kg/mm^2. The new mineral is brittle, with uneven fracture; neither cleavage nor parting was observed. The density calculated based on the empirical formula is 4.356 g/cm^3. In reflected light, gladkovskyite is grayish-white, strongly anisotropic with rotation tints varying from light-grey to brown. Its pleochroism is moderate, from orange-red to dark-red, and bireflectance is very weak, $\Delta R = 0.58$ % (589 nm). The empirical formula of gladkovskyite is $Mn_{1.01}Tl_{0.99}Pb_{0.01}As_{2.86}Sb_{0.13}S_{6.00}$ (based on 11 atoms *pfu*). Prominent features in the Raman spectrum include bands of Mn–S and As–S stretching vibrations as well as numerous low-frequency bands related to phonons. Gladkovskyite is trigonal, *R*31*c*, a = 9.6392(2), c = 6.4560(15) Å, V = 519.49(12) Å^3 and Z = 2. The seven strongest powder X-ray diffraction lines are [d_{obs}, Å (*I*, %) (*hkl*)]: 5.11 (80) (101), 4.83 (70) (110), 3.49 (50) (201), 3.23 (30) (002), 2.86 (100) (–2–11, 211), 2.68 (30) (112), 2.55 (60) (301, 202). The crystal structure of gladkovskyite was refined from the single-crystal X-ray diffraction data to R = 0.0178 for 679 observed reflections with $I_{obs} > 3\sigma(I)$. It contains infinite chains of face-sharing MnS_6 octahedra, TlS_9 polyhedra and pyramidal AsS_3 groups; the structure belongs to the group of seldom occurring cyclic sulfosalts. The new mineral honors Russian geologist Boris Aleksandrovich Gladkovsky who discovered the Vorontsovskoe gold deposit.

Keywords: gladkovskyite, new mineral, sulfosalt, crystal structure, Vorontsovskoe gold deposit, Northern Urals
Received: 24 May 2019; accepted: 18 October 2019; handling editor: F. Laufek
The online version of this article (doi: 10.3190/jgeosci.290) contains supplementary electronic material.

1. Introduction

The actively exploited Vorontsovskoe gold deposit at Northern Urals is unique in Russia with regard to its Tl–Hg–As–Sb mineralization. Our systematic mineralogical investigations of its ores over the last few years revealed a remarkable assemblage of rare minerals, most of which are Tl-sulfosalts. Among them, three minerals are completely new for the science: vorontsovite, ferrovorontsovite (Kasatkin et al. 2018a) and tsygankoite (Kasatkin et al. 2018b). Herein we describe gladkovskyite, the fourth new Tl-sulfosalt from this deposit. In addition, several other potentially new sulfosalts discovered here by our team are currently under study and all of them contain essential thallium. By the richness of its Tl–Hg mineralization, the Vorontsovskoe gold deposit can be undoubtedly put at par with famous Lengenbach in Switzerland or Allchar in the Republic of North Macedonia.

Gladkovskyite (pronouncing: glad kouv ski yait) is named for Boris Aleksandrovitch Gladkovsky (1937–1990), a well-known geologist and prospector of ore and alluvial gold in the Ural Mountains. In 1972, he took the position of chief geologist of the Geological Survey of Northern Urals and started the prospecting of gold ore in the area. The major success of his professional career was the discovery in 1985 by him and his colleagues of the Vorontsovskoe deposit, the biggest in Northern Urals and one of the most significant gold deposits in Russia that yielded extremely interesting Tl-minerals including the one described here.

The new mineral and its name have been approved by the Commission on New Minerals, Nomenclature and

Fig. 1 One of the authors (S.Y.S.) collecting at the bottom of the Northern open pit of the Vorontsovskoe deposit. Photo taken in August 2016 (photo by Roman Palamartchuk).

Classification of the International Mineralogical Association (IMA2018-098). The type specimen is deposited in the collections of the Fersman Mineralogical Museum of the Russian Academy of Sciences, Moscow, Russia with the registration number 5248/1.

2. Occurrence

Gladkovskyite occurs at the Vorontsovskoe gold deposit, approximately 13 km to the south of the city of Krasnotur'insk, Sverdlovskaya Oblast', Northern Urals, Russia. The Vorontsovskoe deposit is situated within a large volcano–plutonic structure comprising polyphase gabbro–diorite–granite Auerbakh Intrusion, volcanic rocks, and volcanogenic sediments of the Krasnotur'inskaya Suite. Rocks of the latter form a monocline, which is gently sloping to the west and tapering to the north. This structure is hosted by limestones, often metamorphosed, with interlayers of tuffites and aleurolites having a thickness of 1 km. The age of magmatites of the Auerbakh Intrusion was determined as mid-Devonian (Krasnobaev et al. 2007). Its emplacement represented a final stage of the development of the intrusive magmatism of the Tagil Volcanic Zone (Fershtater 2013).

The quarry of the Vorontsovskoe deposit uncovered a wedge-like body of volcanoclastic rocks with the predominance of tuffs and tuffaceous sedimentary rocks. The western part of this body is limited by a big tectonic fault. The limestones occur in the lying tectonic contact of the body. Both the volcanogenic sedimentary rocks and the limestones underwent metasomatic processes that resulted in the formation of metasomatites with ore concentrations of gold. The main volume of gold is related to ore breccias, including orpiment–realgar cement. Both the limestones and volcanogenic sedimentary rocks are brecciated. The ore body with economic concentrations of gold has the form of a torch opening upwards (Tcheremisin and Zlotnik-Khotkevitch 1997). The Tl–Hg-bearing sulfosalts are widely distributed, mostly in orpiment–realgar cement of the breccias. The content of these minerals increases in breccias where limestones dominate. A more detailed description of the Vorontsovskoe deposit, its genesis, geology and composition of main ore types can be found elsewhere (Sazonov et al. 1998; Vikentyev et al. 2016; Murzin et al. 2017; Stepanov et al. 2017).

Specimens containing the new mineral were collected in August 2016 by one of the authors (S.Y.S.) in the Severnyi (Northern) open pit of the deposit, 50 m from its western wall, directly at the bottom of the pit (59° 65' 29" N, 60° 21' 33" E) (Fig. 1). Gladkovskyite was found in limestone breccias cemented by major orpiment, realgar, pyrite and baryte, and minor clinochlore, fluorapatite, quartz and talc (Fig. 2). Other minerals directly associating with gladkovskyite include alabandite, bernardite, christite, cinnabar, coloradoite, dalnegroite, gillulyite, gold, hutchinsonite, imhofite, lorandite, metacinnabar, philrothite, rebulite, routhierite, sphalerite, vrbaite and several potentially new Tl-bearing phases currently under investigation.

The mineral association bearing gladkovskyite is one of the most interesting at the Vorontsovskoe deposit. It is connected with a very rich orpiment–realgar type of ores while stibnite, normally relatively abundant at the deposit, is absent here. As a result, one of the most characteristic features of this association is a strong dominance of As

Fig. 2 Limestone breccias with realgar and orpiment, where gladkovskyite was discovered, *in situ*.

Tab. 1 Chemical composition and unit-cell parameters of thallium sulfosalts identified in the association with gladkovskyite at the Vorontsovskoe gold deposit

	Chemical composition, wt.% and *apfu*										
	BRN	CHR	DLN	GIL	HUT	IMH	LOR	PHL	RBL	RTR	VRB
Cu	–	–	–	–	–	–	–	–	–	5.92	–
Zn	–	–	–	–	–	–	–	–	–	0.51	–
Ag	–	–	0.10	–	–	–	–	–	–	0.25	–
Hg	–	34.50	–	–	–	–	–	–	–	38.87	20.42
Tl	21.40	35.73	19.53	29.49	19.14	36.30	58.49	33.17	36.10	19.21	28.52
Pb	0.13	–	10.39	0.19	18.68	–	0.42	0.59	0.29	–	–
As	25.32	12.62	23.13	40.02	31.25	30.02	20.57	34.40	30.63	13.97	20.61
Sb	25.39	–	21.08	1.73	4.73	8.43	0.45	3.94	7.08	1.72	8.57
S	27.98	16.40	26.36	29.52	26.54	25.37	19.37	27.06	25.34	19.03	22.32
Total, wt. %	100.22	99.25	100.59	100.95	100.34	100.12	99.30	99.16	99.44	99.48	100.44
Cu	–	–	–	–	–	–	–	–	–	0.94	–
Zn	–	–	–	–	–	–	–	–	–	0.08	–
Ag	–	–	0.04	–	–	–	–	–	–	0.02	–
Hg	–	1.01	–	–	–	–	–	–	–	1.96	2.94
Tl	0.96	1.02	3.95	2.04	1.02	5.83	0.98	0.97	4.92	0.95	4.02
Pb	0.01	–	2.74	0.01	0.98	–	0.01	0.02	0.04	–	–
As	3.10	0.98	12.77	7.54	4.55	13.14	0.94	2.75	11.39	1.89	7.93
Sb	1.92	–	7.16	0.21	0.42	2.27	0.01	0.19	1.62	0.14	2.03
S	8.01	2.99	34.01	13.00	9.03	25.96	2.06	5.06	22.03	6.01	20.08
Total, *apfu*	14	6	60	22.8	16	47.2	4	9	40	12	37
	Unit-cell parameters*										
Crystal system	Mon.	Mon.	Tricl.	Mon.	Orth.	Mon.	Mon.	Mon.	Mon.	Tetr.	Orth.
a, Å	15.72(2)	6.11(5)	16.33(2)	9.594(2)	10.82(4)	8.776(5)	12.282(2)	8.102(2)	17.35(3)	9.967(5)	13.391(5)
b, Å	8.18(2)	16.2(2)	42.49(3)	5.677(2)	35.39(2)	24.430(3)	11.240(3)	24.845(5)	7.36(2)		23.426(15)
c, Å	10.76(4)	6.11(4)	8.564(5)	21.401(7)	8.22(2)	5.755(2)	6.106(2)	11.785(4)	31.94(4)	11.382(10)	11.294(7)
α, °			95.32(4)								
β, °	91.54(6)	96.7(6)	90.53(4)	100.34(3)		108.40(2)	104.04(2)	132.65(2)	105.12(2)		
γ, °			96.43(6)								
V, Å^3	1383.1(2)	600(10)	5878(3)	1146.5(4)	3147.6(2)	1170.8(2)	817.8(3)	1744.8(2)	3937.4(2)	1131(1)	3543(3)

BRN – bernardite, CHR – chrisite, DLN – dalnegroite, GIL – gillulyite, HUT – hutchinsonite, IMH – imhofite, LOR – lorandite, PHL – philrothite, RBL – rebulite, RTR – routhierite, VRB – vrbaite

* as determined during our study (based on XRD data)

over Sb in the chemical composition of the rare Tl-sulfosalts identified here, all of which are sulfarsenites and not sulfantimonites. The list of all Tl-sulfosalts identified in association with gladkovskyite, their chemical data and refined unit-cell parameters are given in Tab. 1.

3. Physical and optical properties

Gladkovskyite forms dark cherry-red long-prismatic crystals up to 0.2 × 0.1 mm and anhedral grains of the same size embedded in calcite matrix (Figs 3–5). It is transparent and exhibits adamantine luster and red streak. The new mineral is brittle, with uneven fracture. Cleavage and parting were not observed. The new mineral is non-fluorescent. The Vickers hardness (VHN10) is 94 kg/mm^2 (range 91–100 kg/mm^2, n = 3) corresponding to a Mohs hardness of 2–2.5. The density of gladkovskyite could not be measured because of the absence of suitable heavy liquids and paucity of available material. The density calculated based on the empirical formula (Z = 2) and the unit-cell volume determined from the single-crystal X-ray diffraction data is 4.356 g/cm^3.

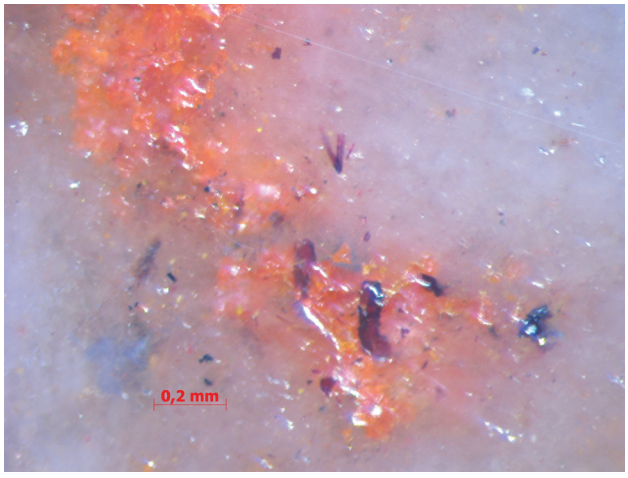

Fig. 3 Dark cherry-red prismatic crystals of gladkovskyite embedded in white calcite matrix with orange-red realgar. Polished section.

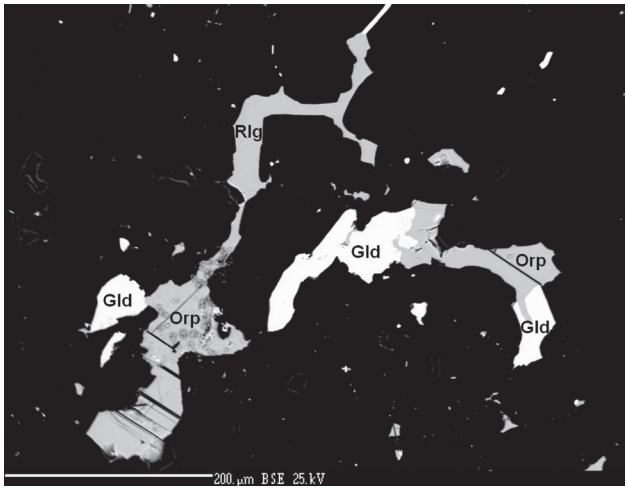

Fig. 4 Gladkovskyite (Gld) grains associated with orpiment (Orp) and realgar (Rlg) in calcite matrix (black); BSE image.

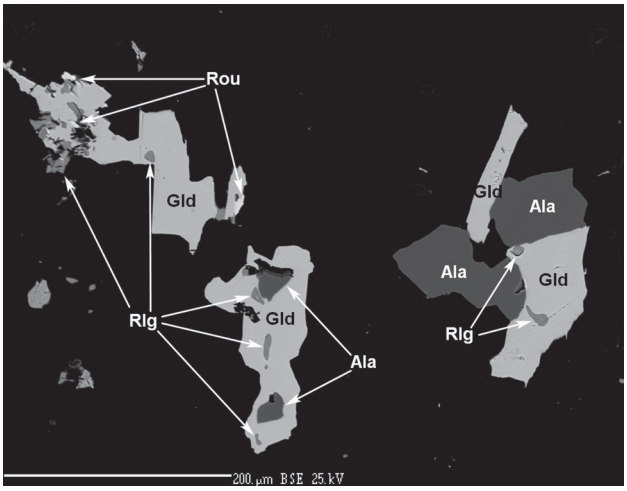

Fig. 5 Gladkovskyite (Gld) crystals and grains associated with alabandite (Ala) and realgar (Rlg) in calcite matrix (black). Routhierite (Rou) occurs as tiny inclusions in gladkovskyite; BSE image.

In reflected light gladkovskyite is grayish-white. It shows a moderate pleochroism, from orange-red to dark-red. The bireflectance is very weak, ΔR = 0.58 % (589 nm). Under crossed polars, the mineral is strongly anisotropic with rotation tints varying from light grey to brown. Internal reflections are not observed. Quantitative reflectance measurements were performed in air relative to a WTiC standard using a Universal Microspectrophotometer UMSP 50 (Opton-Zeiss, Germany). Reflectance values are given in Tab. 2 and plotted in Fig. 6.

4. Raman spectroscopy

The Raman spectrum of gladkovskyite (Fig. 7) was obtained from polished section by a Horiba Labram HR

Tab. 2 Reflectance values of gladkovskyite in % (WTiC standard, measured in air)

λ (nm)	R_1	R_2	λ (nm)	R_1	R_2
400	28.42	21.43	560	22.78	22.65
420	27.59	22.54	580	22.48	22.35
440	27.19	22.94	**589**	**22.38**	**22.25**
460	26.04	23.26	600	22.28	22.17
470	**25.47**	**23.49**	620	21.87	21.64
480	24.91	23.77	640	21.72	21.22
500	24.32	23.97	**650**	**21.70**	**21.04**
520	23.86	23.76	660	21.71	20.85
540	23.73	23.50	680	21.67	20.48
546	**23.50**	**23.42**	700	21.63	20.20

Reflectance percentages for the four COM (Commission on Ore Mineralogy) wavelengths are given in bold

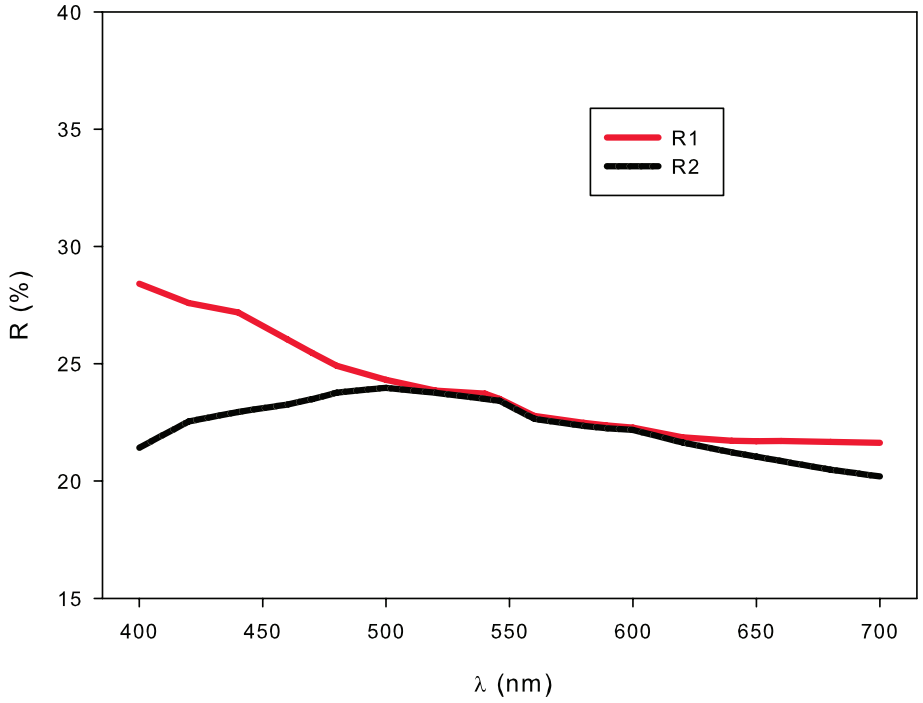

Fig. 6 Reflectance spectra ($R_{max.}$, R_{min}) for gladkovskyite in air.

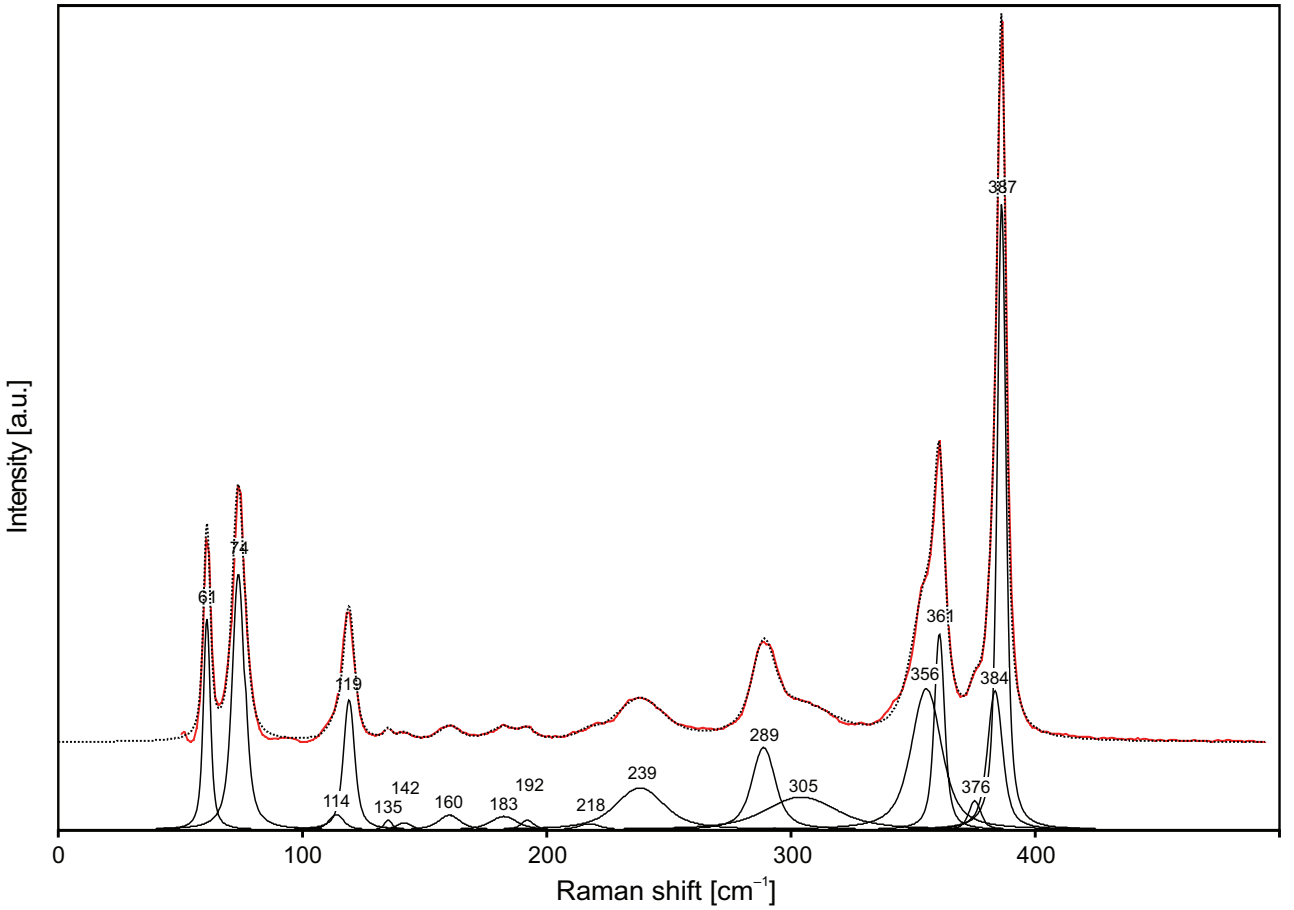

Fig. 7 Raman spectrum of gladkovskyite (excited by 633 nm laser). The experimental spectrum is displayed as solid red line. The black dotted curve matching to the red line is a result of a spectral fit as a sum of individual Voigt peaks shown below the curve.

Evolution spectrometer. This dispersive, edge-filter-based system is equipped with an Olympus BX 41 optical microscope, a diffraction grating with 600 grooves per millimetre, and a Peltier-cooled, Si-based charge-coupled device (CCD) detector. After careful tests with different lasers (473, 532 and 633 nm), the 633 nm He–Ne laser with the beam power of 0.1 mW at the sample surface was selected for spectra acquisition to minimize analytical artefacts. Raman signal was collected in the range of 50–600 cm^{-1} with a 50× objective in the confocal mode, beam diameter was ~2.6 μm and the lateral resolution ~5 μm. No visual damage of the analysed surface was observed at these conditions after the excitation. Wavenumber calibration was done using the Rayleigh line and low-pressure Ne-discharge lamp emissions. The wavenumber accuracy was ~0.5 cm^{-1}, and the spectral resolution was ~2 cm^{-1}. Band fitting was done after appropriate background correction, assuming combined Lorentzian–Gaussian band shapes using Voigt function (PeakFit; Jandel Scientific Software).

A tentative assignment of the Raman bands was made by analogy with simple sulphides. In gladkovskyite, the highest strength show the Mn–S bonds. Bands of M–S stretching vibrations in the Raman spectra of pyrite-type compounds MS_2 (M = Mn, Co, Ni, Cu, Zn) with 3D systems of vertex-sharing MS_6 octahedra are observed in the range 380–500 cm^{-1} (Anastassakis and Perry 1976). For gladkovskyite, which contains 1D system of face-sharing MnS_6 octahedra, somewhat lower frequencies should be expected. This conclusion is in agreement with the positions of the high-frequency bands observed in the Raman spectrum of gladkovskyite in the range 350–400 cm^{-1}.

Raman bands of As–S stretching vibrations in the Raman spectra of orpiment As_2S_3 and realgar AsS are observed in the range 290–360 cm^{-1} (Forneris 1969; Minceva-Sukarova et al. 2003). In these minerals the As–S distances are in the range 2.21–2.31 Å (Morimoto 1954; Mullen and Nowacki 1972). The largest distances correspond to the lowest frequencies of As–S stretching vibrations. In gladkovskyite, the As–S distances are *c*. 2.31 Å. Consequently, the bands at 289 and 305 cm^{-1} in the Raman spectrum of gladkovskyite are attributed to As–S stretching vibrations.

The assignment of Raman bands with wavenumbers below 250 cm^{-1} is ambiguous. Presumably, these bands correspond to mixed soft modes involving bending vibrations, as well as Tl–As and Tl–S stretching vibrations and phonons.

5. Chemical composition

The preliminary semi-quantitative chemical analyses using a scanning electron microscope CamScan 4D equipped with INCA Energy microanalyzer (EDS mode, 20 kV, 5 nA and beam diameter 1 μm) showed the presence of major Mn, Tl, As, S, minor Sb and traces of Pb in gladkovskyite.

Tab. 3 Chemical composition of gladkovskyite

Constituent	wt. %	Range	Stand. Dev.
Mn	8.28	8.16–8.34	0.06
Tl	30.04	29.77–30.44	0.28
Pb	0.23	0.21–0.29	0.04
As	31.80	30.96–32.30	0.57
Sb	2.27	1.13–4.34	1.24
S	28.58	27.95 – 28.85	0.32
Total	101.20		

Quantitative chemical analyses were conducted in wavelength-dispersive (WDS) mode, using a Cameca SX-100 electron microprobe operated at 25 kV and 20 nA with the beam size of 1 μm. Peak-counting times were 20 s for all elements, with one half of the peak time for each background. The following standards, X-ray lines, and crystals (in parentheses) were used: Mn: Mn metal, K_α (LIF); Tl: Tl(Br,I), M_α (PET); Pb: PbSe, M_α (PET); As: pararammelsbergite, L_β (TAP); Sb: Sb, L_β (PET); S: chalcopyrite, K_α (PET). Analytical data are given in Tab. 3 (mean of 7 analyses). No other elements with atomic numbers higher than 8 were detected.

The empirical formula of gladkovskyite, calculated on the basis of 11 atoms pfu is $Mn_{1.01}Tl_{0.99}Pb_{0.01}As_{2.86}Sb_{0.13}S_{6.00}$. The ideal chemical formula is $MnTlAs_3S_6$, which requires 8.16 Mn, 30.17 Tl, 33.25 As, 28.42 S, total 100 wt. %.

6. X-ray crystallography

Single-crystal X-ray diffraction data were collected on a gladkovskyite grain with the dimensions 0.125 × 0.063 × 0.036 mm, which was extracted from the polished section used for electron-microprobe investigations. The data collection was carried out with a Rigaku SuperNova diffractometer, using MoK_α radiation (λ = 0.71073 Å) from a micro-focus X-ray tube collimated and monochromatized by mirror optics and detected by an Atlas S2 CCD detector. Data reduction was done using CrysAlis software (Rigaku 2017).

The crystal structure of gladkovskyite was solved from the diffraction data using SHELXT software (Sheldrick 2015) and refined by the least-squares algorithm of the Jana2006 program (Petříček et al. 2014). The structure refinement smoothly converged to R = 0.0178 for 679 observed reflections, with $I > 3\sigma(I)$, including all atoms refined with harmonic atomic displacement parameters. Data collection and refinement details are listed in Tab. 4, atom coordinates and displacement parameters are given

in Tab. 5, and selected bond lengths in Tab. 6. The CIF file, also containing a block with the reflections, is deposited at the Journal's webpage *www.jgeosci.org*.

Due to lack of material for performing a conventional powder-diffraction experiment we present only a comparison of observed reflections (d_{hkl} spacings and intensities) obtained using a pseudo-Gandolfi scan done on the same instrument as single-crystal data collection and a powder pattern calculated from the structure. The theoretical d_{hkl} and relative intensities were calculated using PowderCell program (Kraus and Nolze 1996). Data are given in Tab. 7.

Tab. 4 Summary of data collection conditions and refinement parameters for gladkovskyite

Formula	$MnTlAs_3S_6$
Crystal system	trigonal
Space group	$P31c$
Unit-cell parameters: a, c [Å]	9.6392(2), 6.4560(15)
Unit-cell volume [Å^3]	519.49(12)
Z	2
Calculated density [g/cm^3]	4.325 (for the formula from structure)
Crystal size [mm]	0.125 × 0.063 × 0.036
Diffractometer	Rigaku SuperNova with Atlas S2 CCD
Temperature [K]	294
Radiation, wavelength [Å]	MoK_α, 0.71073 (50 kV, 30 mA)
θ range for data collection [º]	3.99–26.47
Limiting Miller indices	h = –11→11, k = –11→11, l = –7 → 8
Axis, frame width (º), time per frame (s)	ω, 1.0, 100
Total reflections collected	5407
Unique reflections	689
Unique observed reflections, criterion	679, [$I > 3\sigma(I)$]
Absorption coefficient [mm^{-1}], type	27.32; empirical
T_{min}/T_{max}	0.366/1
Data completeness to θ_{max} (%), R_{int}	98.00, 0.048
Structure refinement	Full-matrix least-squares on F^2
No. of param., restraints, constraints	31, 0, 4
R, wR (obs)	0.0178, 0.0412
R, wR (all)	0.0183, 0.0414
GOF obs/all	1.32, 1.32
Weighting scheme, weights	σ, w =1/(σ^2(I)+0.0004I^2)
Largest diffraction peak and hole (e$^-$/Å^3)	0.76, –0.33
Absolute structure	332 Friedel pairs

6.1. Description of the crystal structure

The crystal structure of gladkovskyite (Figs 8–9) contains five independent atom sites in the asymmetric unit: one Tl, one As, one Mn, and two S. Thallium is coordinated by nine S atoms at an average distance of 3.33 Å in the form of a distorted tricapped trigonal prism. Three shortest Tl–S2 distances, 3.17 Å, are met by three Tl–S2 distances, 3.34 Å long to the prism vertices, and by three Tl–S1 distances of 3.50 Å, and represent horizontally oriented caps to the prism faces (Fig. 10). The bell-shaped form of the prism opens in the direction of the lone electron pair, into an open volume that is limited at the bottom by three S2 atoms at 5.13 Å from Tl, forming the top triangular face of the next Tl prism below. Remaining long Tl–S distances, 5.71 Å and 5.78 Å, form a very open cone around Tl and the three-fold axis on which it is situated. The asymmetry of the coordination environment around Tl site suggests that lone-electron pair on Tl^+ is active.

The high steric activity of the lone pair of Tl reminds that of the TlS_5 configuration in imhofite (Divjaković and Nowacki 1976; Balić-Žunić and Makovicky 1993), but the long connections opposing the 3.85 Å bond in this mineral are one 4.17 Å Tl–S distance and additional 4.75–4.92 Å distances, far shorter than those observed in gladkovskyite. A similar review of the structures of raberite, vrbaite, richardsollyite, and other phases (Makovicky 2018) shows apparent uniqueness of the gladkovskyite arrangement for the lone electron pair accommodation. For example, the interslab Tl–S distance for the pyramidal-coordinated Tl in hutchinsonite (Matsushita and Takeuchi 1994) is 5.20 Å, but the thallium atom has two interslab Tl–S distances to closer S atoms, at 3.331 Å. This makes the polar gladkovskyite structure particularly interesting.

Arsenic is coordinated by three S atoms (one S1 and two S2 atoms, symmetrically related), forming a regular trigonal pyramid (Fig. 10); the lone-electron pair on As

Tab. 5 Atom positions and atomic displacement parameters (in Å^2) for gladkovskyite

Atom	x/a	y/b	z/c	U_{eq}	U^{11}	U^{22}	U^{33}	U^{12}	U^{13}	U^{23}
Tl1	0.666667	0.333333	0.4582(2)	0.03489(13)	0.03481(16)	0.03481(16)	0.0350(3)	0.01740(8)	0	0
As1	0.62288(7)	−0.08195(7)	0.5338(2)	0.0231(2)	0.0235(3)	0.0242(3)	0.0214(3)	0.0117(2)	−0.0008(2)	−0.0001(2)
Mn1	0	0	0.2384(3)	0.0233(4)	0.0248(5)	0.0248(5)	0.0204(8)	0.0124(2)	0	0
S1	0.87194(19)	0.12007(18)	0.4861(3)	0.0230(6)	0.0233(7)	0.0247(7)	0.0234(6)	0.0136(6)	0.0000(5)	0.0001(6)
S2	0.529516(19)	0.03645(19)	0.763361(18)	0.0277(7)	0.0272(8)	0.0394(9)	0.0224(8)	0.0210(7)	0.0012(6)	0.0030(6)

Tab. 6 Selected interatomic distances (Å) in the structure of gladkovskyite

Tl1–As1	3.8407(8)
Tl1–As1^{i}	3.8407(7)
Tl1–As1^{ii}	3.8407(11)
Tl1–As1^{iii}	3.7957(18)
Tl1–As1^{iv}	3.7957(19)
Tl1–As1^{v}	3.7957(18)
Tl1–S1	3.499(2)
Tl1–S1^{i}	3.499(2)
Tl1–S1^{ii}	3.499(2)
Tl1–S2	3.1678(11)
Tl1–S2^{i}	3.1678(11)
Tl1–S2^{ii}	3.1678(11)
Tl1–S2^{iii}	3.3351(6)
Tl1–S2^{iv}	3.3351(6)
Tl1–S2^{v}	3.3351(6)
As1–S1^{iv}	3.826(3)
As1–S2	2.3101(12)
As1–S2^{iv}	2.3140(14)
Mn1–S1	2.617(2)
Mn1–S1^{viii}	2.617(2)
Mn1–S1^{xi}	2.617(2)
Mn1–S1^{x}	2.635(2)
Mn1–S1^{iv}	2.635(2)
Mn1–S1^{xii}	2.635(2)

Symmetry codes: (i) –*y*+1, *x*–*y*, *z*; (ii) –*x*+*y*+1, –*x*+1, *z*; (iii) *y*+1, *x*, *z*–1/2; (iv) *x*–*y*, –*y*, *z*–1/2; (v) –*x*+1, –*x*+*y*+1, *z*–1/2; (vi) *x*–y, –*y*, *z*+1/2; (vii) *y*+1, *x*–1, *z*+1/2; (viii) –*y*+1, *x*–y–1, *z*; (ix) –*x*+1, –*x*+y, *z*–1/2; (x) *y*+1, *x*–1, *z*–1/2; (xi) –*x*+*y*+2, –*x*+1, *z*; (xii) –*x*+2, –*x*+*y*+1, *z*–1/2; (xiii) –*x*+2, –*x*+*y*+1, *z*+1/2

Tab. 7 Calculated powder X-ray data for gladkovskyite (only diffractions with $I_{rel.}$ > 5% are listed) compared with experimental data obtained from pseudo-Gandolfi scan

$I_{rel.calc.}$ (%)	$d_{calc.}$ (Å)	*h*	*k*	*l*	$I_{obs.}$ (%)	$d_{obs.}$ (Å)
7	8.348	1	0	0		
73	5.107	1	0	1	80	5.11
88	4.820	1	1	0	70	4.83
67	3.505	2	0	1	50	3.49
25	3.228	0	0	2	30	3.23
6	3.115	2	1	0	3	3.13
8	3.011	1	0	2		
100	2.835	–2	–1	1	100	2.86
47		2	1	1		
36	2.783	3	0	0	10	2.77
33	2.682	1	1	2	30	2.68
9	2.555	3	0	1	60	2.55
56		2	0	2		
30	2.410	2	2	0	10	2.41
9	2.256	2	1	2	10	2.24
7		–2	–1	2		
9	2.179	3	1	1	5	2.18
15	2.108	3	0	2	15	2.09
13	2.040	1	0	3		
10	1.881	3	1	2		
16	1.836	–3	2	1	20	1.83
16		3	2	1		
11	1.822	4	1	0		
19	1.778	–2	1	3		
17	1.753	4	0	2		
16	1.616	5	0	1		
7	1.576	3	1	3		

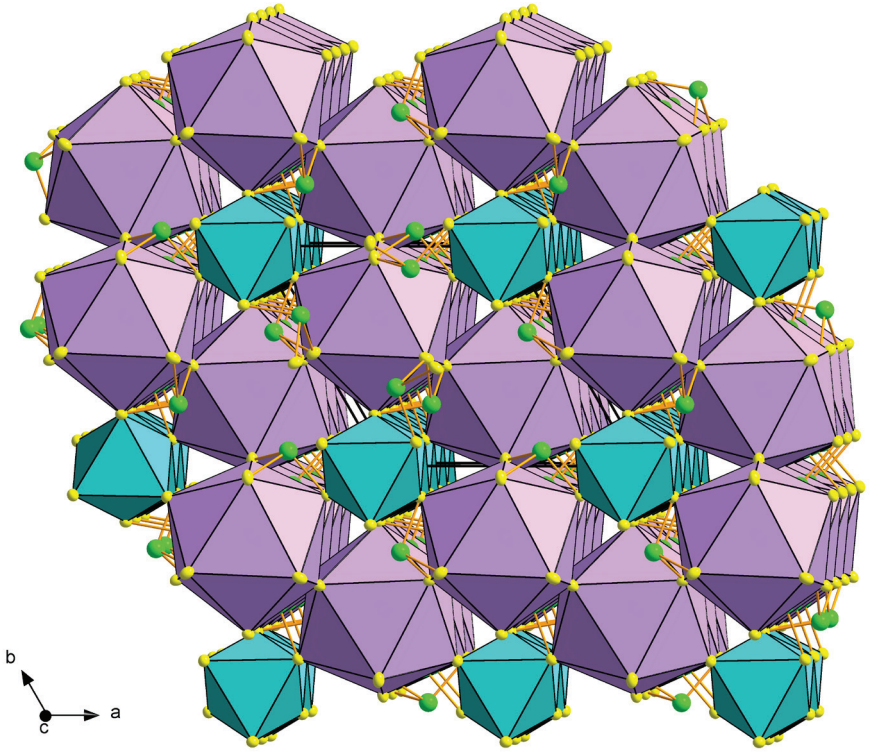

Fig. 8 The crystal structure of gladkovskyite projected approximately along [001], slightly inclined. Tl polyhedra (CN9) are purple, Mn octahedra are intense-blue, AsS_3 pyramids are in ball-and-stick representation (As green, S yellow). All S atoms are displayed as thermal ellipsoids.

is stereoactive, located nearly perpendicular to [001] (Fig. 9). Arsenic pyramids form [001] chains *via* shared S atoms.

Manganese is coordinated by six S atoms at an average distance of 2.63 Å as a nearly regular MnS_6 octahedron (Fig. 10). These octahedra share triangular faces and form [001] columns. Periodicity parallel to [001] is as follows: two Mn octahedrons match two As pyramids with different orientation, but only one Tl polyhedron. The alternating polyhedron along [001]

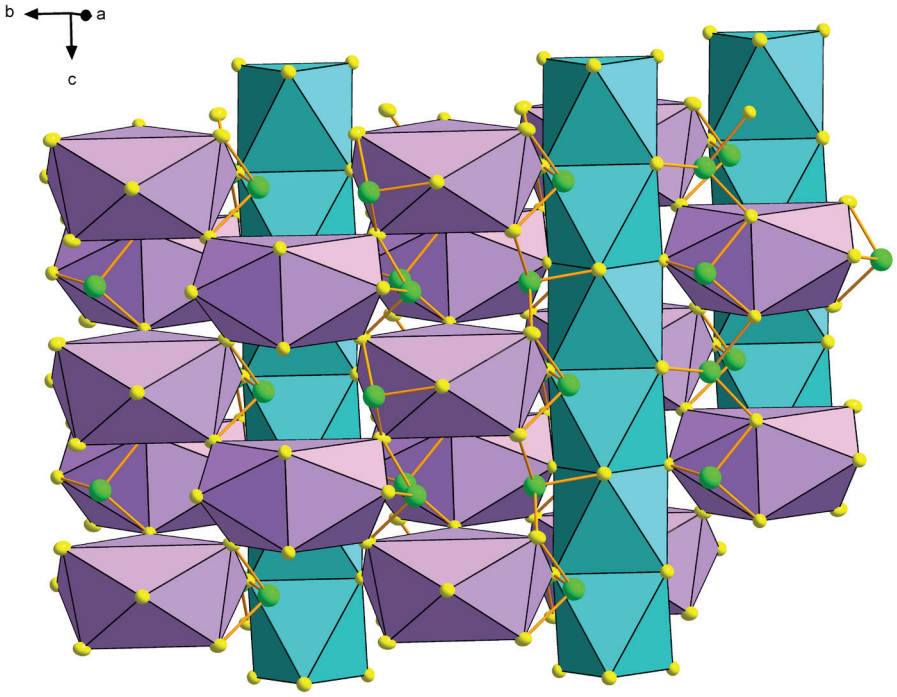

Fig. 9 Thallium columns (violet) alternating Mn columns (azure) in the crystal structure of gladkovskyite. Note the interspaces for downward projecting lone electron pairs of Tl, as well as cavities due to stereoactivity of the electron lone-pair on As (green). All S atoms are displayed as thermal ellipsoids.

is occupied by the lone electron pair of Tl. Polarity of this structure parallel to [001] is primarily caused by the steric activity of thallium.

The *c* parameter of gladkovskyite is determined by the periodicity of the column of Mn octahedra. Orientation of As coordination pyramids is adjusted to the approximate 2 × 3.3 Å period of the Mn polyhedral chain. Plane group symmetry of an individual *z* level of atoms is approaching *p*31*m*, although when complete AsS_3 groups are considered it is *p*3, and when complete chains of AsS_3 pyramids are included, it becomes *P*31*c* for the entire structure.

7. Discussion

7.1. Remarks on the crystal structure

The structure of gladkovskyite belongs to the small group of 'cyclic sulfosalt structures' of which zinkenite is the most well-known representative. Among members of this group, gladkovskyite distinguishes itself by the low (only threefold) multiplicity of its rotation symmetry.

The structure of $Bi_{6.88}Cl_{3.36}S_{8.64}$ is metrically closest to gladkovskyite (Poudeu and Ruck 2006), but its structure model is actually a sub-cell of $Bi_4Cl_2S_5$ with a = 19.804 Å and c = 12.359 Å, space group *R*-3*H* (Krämer 1979). This structure has hexagonal channels filled by Bi. The channels are surrounded by a ring of bicapped trigonal prisms of Bi. These prisms are interconnected with the

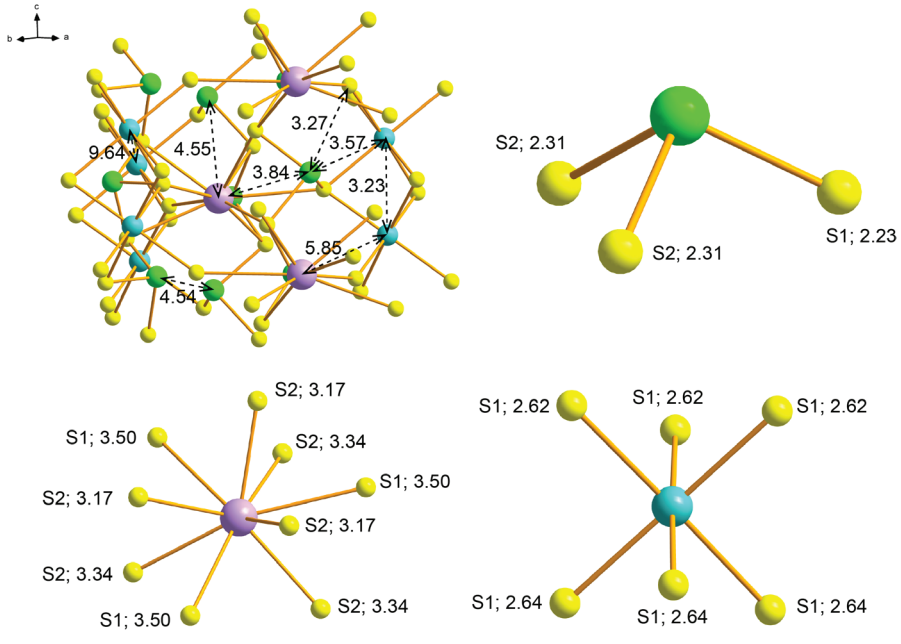

Fig. 10 The Tl–S bonds, selected interatomic distances and coordination polyhedra in the structure of gladkovskyite. Tl is violet, Mn azure, As green, S yellow. Distances are given in Å.

prisms surrounding the adjacent channel, forming a narrow double-ribbon composed of four Bi coordination polyhedra. One *z* atomic level has symmetry *p*3.

The structure of $Cu_{7.4}Bi_6Cl_7Se_{12}$ (Heerwig and Ruck 2009) has channels of hexagonal shape limited by Cl and filled by fractionally occupied Cu sites and central Cl atoms. They are surrounded by a ring of split coordination pyramids of Bi which, two and two together, mimic bicapped trigonal prisms with Se and Cl ligands, with $CuSe_4$ attached to them sideways. The latter polyhedra configure a ring of three Cu coordination tetrahedra around threefold axes of the space group *P*6/*m*. Although the unit cell given is only *a* = 15.058 Å and *c* = 4.014 Å, the complex rings of Bi polyhedra suggest that it is an overlap structure and at least the *c* parameter in this structure might be doubled.

The largest structure of this structural group, zinkenite, idealized as $Cu_{0.7}Pb_{9.7}Sb_{21.3}S_{42}$ (Biagioni et al. 2018, and references therein) has a pronounced hexagonal sub-cell (*a* = 22.122 Å, *c* = 4.321 Å, substructure symmetry $P6_3$), whereas the true cell, true symmetry and twinning have been variously interpreted. The latter reference suggests a triclinic true cell with *c* equal to 8.6475 Å. Hexagonal channels have mixed (Pb,Sb) walls, superficially reminding us of the previous structure. This, and the problems of bond distribution in the rods and channel envelopes, indicates clearly a doubled or a multiple *c* parameter.

This short review indicates a complex structural situation with unresolved multiplicity of overlapping motifs and of the (pseudo)hexagonal *c* parameter in half of these cyclic structures. These factors prevent finding a possible common denominator of this structure group, and possible topological relations to the well-resolved structure of gladkovskyite. The most obvious difference, the 2 × 3.2 Å *c*-axis periodicity of gladkovskyite vs. the *n* × 4.2 Å type of periodicity in the quoted examples, suggests important structural differences between these two end-members of structure arrangements.

7.2. Remarks on the origin

The important feature of the mineral association, where gladkovskyite was found, is a wide distribution of alabandite which served as the main source of Mn. The character of relationship between gladkovskyite and alabandite observed in thin sections allows us to conclude that the latter is replaced by the former: one can easily see relics of alabandite in gladkovskyite (see Fig. 5). A similar relationship was observed between alabandite and tsygankoite, another Mn–Tl mineral recently described from Vorontsovskoe (Kasatkin et al. 2018b).

Similarly to the majority of other Tl-sulfosalts recorded at the Vorontsovskoe deposit, gladkovskyite was discovered in the orpiment–realgar-bearing cement of ore breccias with dominant limestones and marbles. The confinement of Tl mineralization to carbonate sedimentary rocks is characteristic of the Carlin deposit in Nevada (Dickson et al. 1979; Radtke 1985), Allchar in Macedonia (Janković and Jelenković 1994; Volkov et al. 2006), Lengenbach in Switzerland (Hettman et al. 2014; Raber and Roth 2018), and Jas Roux in France (Johan and Mantienne 2000). The mobilization of thallium into the hydrothermal systems was possible due to low-temperature metasomatic processes initiated by a magmatic source in the Carlin deposit (Silitoe and Bonham 1990; Cline et al. 2003; Cline et al. 2005), Allchar (Volkov et al. 2006) and Jas Roux (Johan and Mantienne 2000), or low-temperature metamorphogenic fluids in Lengenbach (Hofmann and Knill 1996). At the Vorontsovskoe deposit, mechanisms of thallium concentration have not been determined unambiguously yet, but we believe that they were related to the interaction between post-magmatic hydrothermal solutions and carbonate rocks. The latter could perform geochemical trap for ore-bearing solutions and, therefore, became a place of concentration of thallium and formation of Tl-bearing sulfosalts. Location of the Vorontsovskoe deposit in the ore-magmatic system connected with Auerbakh intrusive (Minina 1994), and petrographic and structural features of ore breccias containing orpiment–realgar cement (Stepanov et al. 2017) confirm that in case of Vorontsovskoe deposit the main volume of mineral-forming fluids and hydrotherms was connected with intrusive activity, similar to Carlin and Allchar.

It is noteworthy that Vorontsovskoe is a multiple-stage deposit and contains metasomatites (skarns, quartz–sericite rocks and jasperoids), which were formed under different temperatures (Tcheremisin and Zlotnik-Khotkevitch 1997). This resulted in a particular mineral sequence. The formation of the cement of ore breccias at earlier, high-temperature stages was accompanied by the crystallization of primary sulfides such as pyrite, arsenopyrite, stibnite, sphalerite, alabandite etc. The gradual decrease of temperature led to the crystallization of realgar and orpiment followed by the formation of the main volume of Tl–Pb–Hg-bearing sulfosalts. Their late character is observed in the pseudomorphs: stibnite is replaced by parapierrotite, realgar by chabourneite and dalnegroite, and alabandite by tsygankoite and gladkovskyite. As noted above, the crystallization of sulfarsenites including gladkovskyite was connected with the saturation of the ore-forming environment by As at a very low activity of Sb.

Summarizing, it can be concluded that the following factors determined the formation of gladkovskyite: development of low-temperature metasomatic processes in sedimentary carbonate rocks rich in Tl; multi-stage mineral sequence with the formation of sulfide associa-

tion containing alabandite at earlier stages and Tl-bearing sulfarsenites paragenesis (gladkovskyite, bernardite, chrisite, dalnegroite, gillulyite, hutchinsonite, imhofite, lorandite etc.) at later stages; strong dominance of As over Sb in the mineral-forming environment.

Acknowledgements. Comments by František Veselovský and Tonči Balić-Žunić as well as the handling editor František Laufek helped to improve the manuscript. This work was financially supported by the project No. LO1603 under the Ministry of Education, Youth and Sports, National sustainability program I of Czech Republic for J.P.

Electronic supplementary material. Supplementary crystallographic data for this paper are available online at the Journal web site (*http://dx.doi.org/10.3190/jgeosci.290*).

References

Anastassakis E, Perry CH (1976) Light scattering and IR measurements in XS_2 pyrite-type compounds. J Chem Phys 64: 3604–3609

Balić-Žunić T, Makovicky E (1993) Contributions to the crystal chemistry of thallium sulphosalts. I. The O–D nature of imhofite. Neu Jb Mineral, Abh 165: 317–330

Biagioni C, Bindi L, Moëlo Y (2018) Another step toward the solution of the real structure of zinkenite. Z Kristallogr 233: 269–277

Cline JS, Stuart FM, Hofstra AH, Premo W, Riciputi L, Tosdal RM, Tretbar R (2003) Multiple sources of ore-fluid components at the Getchell Carlin-type gold deposit, Nevada, USA. In: Eliopoulos DG (ed) Mineral Exploration and Sustainable Development. Millpress, Rotterdam, pp 965–968

Cline JS, Hofstra AH, Muntean JL, Tosdal RM, Hickey KA (2005) Carlin-type gold deposits in Nevada – critical geological characteristics and viable models. Econ Geol 100: 371–405

Dickson FW, Radtke AS, Peterson JA (1979) Ellisite, Tl_3AsS_3, a new mineral from the Carlin gold deposit, Nevada, and associated sulfide and sulfosalt minerals. Amer Miner 64: 701–707

Divjaković V, Nowacki W (1976) Die Kristallstruktur von Imhofit, $Tl_{5.6}As_{15}S_{25.3}$. Z Kristallogr 144: 323–333 (in German)

Fershtater GB (2013) Paleozoic Intrusive Magmatism of Middle and South Urals. Ural Branch of the Russian Academy of Sciences, Yekaterinburg, pp 1–368 (in Russian)

Forneris R (1969) Infrared and Raman spectra of realgar and orpiment. Amer Miner 54: 1062–1074

Heerwig A, Ruck M (2009) $Cu_9Bi_9S_{16}Cl_8$ and $Cu_{7.4}Bi_6Se_{12}Cl_7$ frameworks of polyhedra with dichalcogenide bridges and mobile copper (I) cations. Z Anorg Allg Chem 635: 2162–2169

Hettmann K, Kreissig K, Rehkämper M, Wenzel T, Mertz-Kraus R, Markl G (2014) Thallium geochemistry in the metamorphic Lengenbach sulfide deposit, Switzerland: thallium-isotope fractionation in a sulfide melt. Amer Miner 99: 793–803

Hofmann BA, Knill MD (1996) Geochemistry and genesis of the Lengenbach Pb–Zn–As–Tl–Ba-mineralization, Binn Valley, Switzerland. Miner Depos 31: 319–339

Janković S, Jelenković R (1994) Thallium mineralization in the Allchar Sb–As–Tl–Au deposit. Neu Jb Mineral, Abh 167: 283–297

Johan Z, Mantienne J (2000) Thallium-rich mineralization at Jas Roux, Hautes-Alpes, France: a complex epithermal, sediment-hosted, ore-forming system. J Czech Geol Soc 45: 63–77

Kasatkin AV, Nestola F, Agakhanov AA, Škoda R, Karpenko VY, Tsyganko MV, Plášil J (2018a) Vorontsovite, $(Hg_5Cu)_{\Sigma 6}TlAs_4S_{12}$, and ferrovorontsovite, $(Fe_5Cu)_{\Sigma 6}TlAs_4S_{12}$: the Tl- and Tl–Fe-analogues of galkhaite from the Vorontsovskoe gold deposit, Northern Urals, Russia. Minerals 8: 185

Kasatkin AV, Makovicky E, Plášil J, Škoda R, Agakhanov AA, Karpenko VY, Nestola F (2018b) Tsygankoite, $Mn_8Tl_8Hg_2(Sb_{21}Pb_2Tl)_{\Sigma 24}S_{48}$, a new sulfosalt from the Vorontsovskoe gold deposit, Northern Urals, Russia. Minerals 8: 218

Krämer V (1979) Structure of the bismuth chloride sulphide $Bi_4Cl_2S_5$. Acta Cryst B35: 139–140

Krasnobaev AA, Fershtater GB, Bogomolov ES, Larionov AN, Berezhnaya NG (2007) Auerbakh Massif: zircons, age, polychronicity. 2006 Yearbook of the Institute of Geology and Geochemistry. Ural Branch of the Russian Academy of Sciences, Yekaterinburg, pp 191–196 (in Russian)

Kraus W, Nolze G (1996) POWDER CELL – a program for the representation and manipulation of crystal structures and calculation of the resulting X-ray powder patterns. J Appl Cryst 29: 301–303

Makovicky E (2018) Modular crystal chemistry of thallium sulfosalts. Minerals 8: 478

Matsushita Y, Takéuchi Y (1994) Refinement of the crystal structure of hutchinsonite, $TlPbAs_5S_9$. Z Kristallogr 209: 475–478

Minceva-Sukarova B, Jovanovski G, Makreski P, Soptrajanov B, Griffith W, Willis R, Grzetic I (2003) Vibrational spectra of $M^IM^{III}S_2$ type synthetic minerals (M^I = Tl or Ag and M^{III} = As or Sb). J Mol Struct 651–653: 181–189

Minina OV (1994) The Auerbakh Complex ore-magmatic system of the Middle Ural. Native Geology 7: 17–23

Morimoto N (1954) The crystal structure of orpiment (As_2S_3) refined. Mineral J 1: 160–169

Mullen DJE, Nowacki W (1972) Refinement of the crystal structures of realgar, AsS and orpiment, As_2S_3. Z Kristallogr 136: 48–65

Murzin VV, Naumov EA, Azovskova OB, Varlamov DA, Rovnushkin MY, Pirajno E (2017) The Vorontsovskoe Au–Hg–As ore deposit (Northern Urals, Russia): geological setting, ore mineralogy, geochemistry, geochronology and genetic model. Ore Geol Rev 85: 271–298

Petříček V, Dušek M, Palatinus L (2014) Crystallographic computing system Jana2006: general features. Z Kristallogr 229: 345–352

Poudeu PFP, Ruck M (2006) The intergrowth structure of $Ag_{1.2}Bi_{17.6}S_{23}Cl_8$ and its relation to the tubular structure of $Bi_{6+\delta}S_{6+3\delta}Cl_{6-3\delta}$ and the pavonite homologue $Ag_{3x}Bi_{5-3x}S_{8-6x}Cl_{6x-1}$. J Solid State Chem 179: 3636–3644

Raber T, Roth P (2018) The Lengenbach quarry in Switzerland: classic locality for rare thallium sulfosalts. Minerals 8: 409

Radtke AS (1985) Geology of the Carlin Ore Deposit, Nevada. USGS Professional Paper 1267: pp 1–124

Rigaku (2017) CrysAlis CCD and CrysAlis RED. Rigaku-Oxford Diffraction Ltd, Yarnton, Oxfordshire, UK

Sazonov VN, Murzin VV, Grigor'ev NA (1998) Vorontsovsk gold deposit: an example of Carlin-type mineralization in the Urals, Russia. Geol Ore Deposits 40: 139–151.

Sheldrick GM (2015) SHELXT – integrated space-group and crystal-structure determination. Acta Cryst A71: 3–8

Silitoe RH, Bonham HF (1990) Sediment-hosted gold deposits: distal products of magmatic–hydrothermal systems. Geology 18: 157–161

Stepanov SY, Sharpenok LN, Antonov AV (2017) Fluid-explosive breccias of the Vorontsovskoe gold deposit (the North Urals). Zap Ross Mineral Obsh 1: 59–70 (in Russian)

Tcheremisin AA, Zlotnik-Khotkevitch (1997) Vorontsovskoe gold deposit. Ores and Metals 1: 59–70 (in Russian)

Vikentyev IV, Tyukova EE, Murzin VV, Vikentyeva OV, Pavlov LG (2016) The Vorontsovsk Gold Deposit. Geology, Gold Modes, Genesis. Fort Dialog-Iset, Yekaterinburg, pp 1–204 (in Russian)

Volkov AV, Serafimovski T, Kochneva NT, Tomson IN, Tasev G (2006) The Alshar Epithermal Au–As–Sb–Tl deposit, Southern Macedonia. Geol Ore Deposits 48: 175–192